Article

A Molecular Tweezer for Lysine and Arginine

Michael Fokkens, Thomas Schrader, and Frank-Gerrit Klrner

J. Am. Chem. Soc., **2005**, 127 (41), 14415-14421• DOI: 10.1021/ja052806a • Publication Date (Web): 27 September 2005

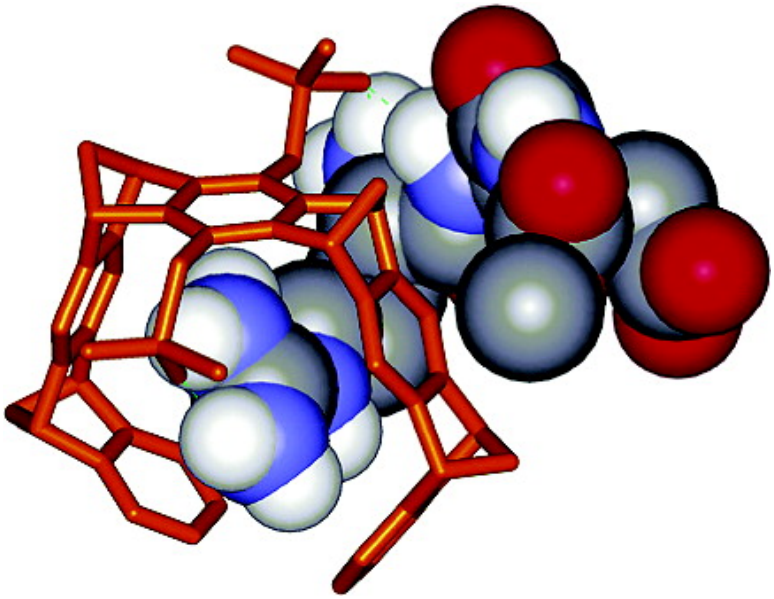

J|A|C|S
ARTICLES
Published on Web 09/27/2005

A Molecular Tweezer for Lysine and Arginine

Michael Fokkens, Thomas Schrader,*,† and Frank-Gerrit Klärner*,‡

Contribution from the Philipps-Universität Marburg, Fachbereich Chemie, Hans-Meerwein-Strasse, 35032 Marburg, Germany, and Universität Duisburg-Essen, Institut für Organische Chemie, Universitätsstrasse 5, 45117 Essen, Germany

Received April 29, 2005; E-mail: schradet@staff.uni-marburg.de

Abstract: Lysine and arginine play a key role in numerous biological recognition processes controlling, inter alia, gene regulation, glycoprotein targeting and vesicle transport. They are also found in signaling peptide sequences responsible, e.g. for bacterial cell wall biosynthesis, Alzheimer peptide aggregation and skin regeneration. Almost none of all artificial receptor structures reported to date are selective and efficient for lysine residues in peptides or proteins. An artificial molecular tweezer is introduced which displays an exceptionally high affinity for lysine ($K_a \approx 5000$ in neutral phosphate buffer). It features an electron-rich torus-shaped cavity adorned with two peripheral anionic phosphonate groups. Exquisite selectivity for arginine and lysine is achieved by threading the whole amino acid side chain through the cavity and subsequent locking by formation of a phosphonate−ammonium/guanidinium salt bridge. This pseudorotaxane-like geometry is also formed in small basic signaling peptides, which can be bound with unprecedented affinity in buffered aqueous solution. NMR titrations, NOESY and VT experiments as well as ITC measurements and Monte Carlo simulations unanimously point to an enthalpy-driven process utilizing a combination of van der Waals interactions and substantial electrostatic contributions for a conformational lock. Since DMSO and acetonitrile compete with the amino acid guest inside the cavity, a simple change in the cosolvent composition renders the whole complexation process reversible.

Introduction

Lysine and arginine residues in peptides and proteins play a vital role in biological processes. Proteins ready for proteasomic degradation are ubiquitinylated at their lysine residues (kiss of death),[1] histones are specifically lysine-ϵ-*N*-acetylated (Gcn5) and deacetylated (Rpd3) to activate or repress transcription (gene regulation).[2] RNA recognition processes controlling transcription often rely on complex formation with arginine-rich regulatory proteins such as *tat* and *Rev* protein.[3] Lysine is also a common determinant for mannose phosphorylation of lysosomal proteins (glycoprotein targeting).[4] Proteins with *C*-terminal dilysine signals are targeted to and retained in the endoplasmic reticulum.[5] Even the intracellular vesicle transport is regulated via dilysine motifs in cargo proteins.[6] These examples highlight the challenge and also the opportunity to develop artificial selective and efficient receptors for lysine and arginine, because they might allow control of, inter alia, gene regulation, glycoprotein targeting and vesicle transport by an external stimulus.

The natural antibiotic vancomycin recognizes the Lys-D-Ala-D-Ala sequence, an important building block for bacterial cell walls.[7] The RGD sequence, on the other hand, is a key recognition element found in many proteins that interact with integrins on cell surfaces.[8] In the central part of Aβ the KKLVFF sequence has recently been identified as the nucleation site which initiates aggregation and subsequent plaque formation in Alzheimer's disease.[9] It was also lately discovered, that the lysine-rich pentapeptide KTTKS sends a signal to the injured cell to regenerate its own collagen, with potential applications in the anti-aging technology.[10] Octaarginine tails in cell-penetrating peptides facilitate membrane transport of an ever-increasing number of drugs, exceeding their own size by up to 100-fold.[11] Finally, the combination of an integrin-binding RGD-cyclopeptide with a hexadecalysine DNA binding domain leads to peptidic minivectors for efficient gene transport.[12] An external agent capable of selective lysine and arginine recognition in a peptidic framework could therefore interfere with bacterial cell wall biosynthesis, Alzheimer peptide aggregation and skin regeneration, to name just a few.

† Philipps-Universität Marburg.
‡ Universität Duisburg-Essen.

(1) Burger, A. M.; Seth, A. K. *Eur. J. Cancer* **2004**, *40*, 2217−2229.
(2) Dutnall, R. N.; Tafrov, S. T.; Sternglanz, R.; Ramakrishnan, V. *Cell* **1998**, *94*, 427−438; Taunton, J.; Hassig, C. A.; Schreiber, S. L. *Science* **1996**, *272*, 408−411.
(3) Ellington, A. D. *Curr. Biol.* **1993**, *3*, 375−377; Varani, G. *Acc. Chem. Res.* **1997**, *30*, 189−195.
(4) Cuozzo, J. W.; Sahagian, G. G. *J. Biol Chem.* **1994**, *269*, 14490−14496.
(5) Andersson, H.; Kappeler, F.; Hauri, H. P. *J. Biol. Chem.* **1999**, *274*, 15080−15084.
(6) Yang, J. S.; Lee, S. Y.; Gao, M.; Bourgoin, S.; Randazzo, P. A.; Premont, R. T.; Hsu, V. W. *J. Cell Biol.* **2002**, *159*, 69−78.
(7) Williams, D. H.; Bardsley, B. *Angew. Chem., Int. Ed.* **1999**, *38*, 1173−1193.
(8) Hynes, R. O. *Cell* **1992**, *69*, 11−25.
(9) Tjernberg, L. O.; Lilliehook, C.; Callaway, D. J. E.; Naslund, J.; Hahne, S.; Thyberg, J.; Terenius, L.; Nordstedt, C. *J. Biol. Chem.* **1997**, *272*, 12601−12605.
(10) Guttman, C. *Dermatol. Times* **2002**, September 1st.
(11) Eirîksdôttir, E.; Myrberg, H.; Hansen, M.; Langel, Ü. *Drug Des. Rev.−Online* **2004**, *1*, 161−173.
(12) Cooper, R. G.; Harbottle, R. P.; Schneider, H.; Coutelle, C.; Miller, A. D. *Angew. Chem., Int. Ed.* **1999**, *111*, 2128−2132.

Artificial receptors, which bind selectively to lysine or arginine, especially in a peptidic environment, should be of considerable interest as potential new pharmaceuticals, as well as molecular probes for some of the related biological processes. Surprisingly, the number of different binding motifs for both amino acids is still very limited. Most synthetic receptors targeting basic amino acids contain crown ethers, although in buffered aqueous solution, their ammonium/guanidinium affinity is almost immeasurably small (K_a < 10 M^{-1}). Kinoshita and König combined two crown ether moieties and achieved a distance-dependent affinity tuning for diammonium and (di)-lysine guests in methanol.[13] Kim and Ahn developed tripodal benzene trisoxazolines with very high alkylammonium affinity in chloroform.[14] Certain calix[4]- and -[5]arenes have also been discovered to include lysine and arginine side chains.[15] Among the best arginine binders reported to date are the polyanionic cyclophanes designed by the Dougherty group, which extensively utilize π−cation interactions.[16] Powerful hydrogen bonds are the basis of Bell's polyaza-aromatic hexagonal lattice receptors for arginine.[17] In yet an alternative bioorganic approach Famulok et al. developed a highly effective arginine binder by in vitro evolution of RNA aptamers.[18]

However, almost none of these artificial receptors is selective and efficient for lysine residues in peptides or proteins.[19] In this report we present a new water-soluble molecular tweezer (see Figure 1), featuring a rigid torus-shaped unpolar cavity adorned with two rotatable peripheral anionic phosphonate groups. The molecule was designed as a suitably preorganized cleft with a high electron density on its inner surface, which should facilitate the complete desolvation of tetrahedral alkylammonium ions. Our expectations were supported by weak binding of dialkylammonium ions by the parent compound in organic solvents.[20]

Results and Discussion

Nine annulated six-membered rings are formed in the key step of a Diels−Alder cycloaddition between the dienophile centerpiece and two diene walls. Subsequent DDQ oxidation, followed by LAH-cleavage of the *O*-acetyl groups furnishes the hydroquinone clip precursor.[21] It is doubly esterified with methanephosphonic acid dichloride and displacement of the remaining chloride with methanol. The resulting methyl phosphonate can be most conveniently purified by chromatography.

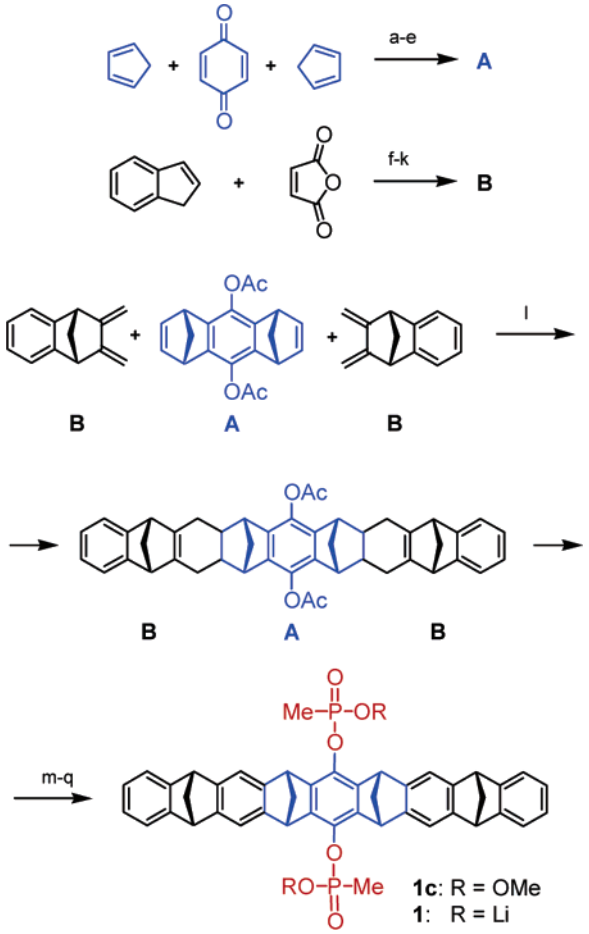

Figure 1. Synthetic route to the new molecular bisphosphonate tweezer **1**. (a) MeOH, 79%; (b) NEt_3, 99%; (c) *p*-benzoquinone, 82%; (d) cyclopentadiene, 99%; (e) Ac_2O, py, DMAP, 96%; (f) hydroquinone, tetraline, 22%; (g) AcCl, 97%; (h) NaOMe, 98%; (i) $LiAlH_4$, 94%; (j) PPh_3Cl_2, imidazole, py, 87%; (k) KOH, 18-crown-6, 90%; (l) NEt_3, sealed tube, 4d 170 °C, 71%; (m) DDQ, 83%; (n) $LiAlH_4$, 98%; (o) $MePOCl_2$, TEA, 71%; (p) MeOH, 79%; (q) LiBr, 80%.

Final dealkylation is mildly effected with LiBr and affords the receptor molecule as lithium salt. It is very well soluble in a broad range of polar solvents (from DMSO to water) and undergoes only very weak self-association even in water as evidenced by a dilution and a variable-temperature experiment.

The propensity of its inner cavity to accommodate unpolar guests is highlighted by the efficient self-inclusion of the methylphosphonate ester group in **1c** prior to the final dealkylation. In a fast equilibrium, only one methyl ester is inserted into the cavity at a given time, rendering the whole clip strongly nonsymmetric. Thus, an average upfield shift of 1.5 ppm results for both methyl ester groups; however, after nucleophilic ester cleavage, the host spectrum reappears simple and perfectly symmetric, without any group inserted into the cavity, i.e., ready to receive guests (Figure 2).

Contrary to a water-soluble clip which binds only flat aromatic cations,[22] the new tweezer induces marked upfield shifts of CH guest protons in primary and secondary ammonium derivatives. Nonlinear regression analysis of the binding isotherms resulting from NMR dilution titrations correspond to

(13) Fuji, K.; Tsubaki, K.; Tanaka, K.; Hayashi, N.; Otsubo, T.; Kinoshita, T. *J. Am. Chem. Soc.* **1999**, *121*, 3807−3808; Mandl, C. P.; König, B. *J. Org. Chem.* **2005**, *70*, 670−674.
(14) (a) Ahn, K.-H.; Kim, S.-G.; Jung, J.; Kim, J.; Chin, J.; Kim, K. *Chem. Lett.* **2000**, 170−171. (b) Chin, J.; Walsdorff, C.; Stranix, B.; Oh, J.; Chung, H. J.; S.-M. Park, Kim, K. *Angew. Chem., Int. Ed.* **1999**, *38*, 2756−2759.
(15) Douteau-Guével, N.; Perret, F.; Coleman, A.; J.-P, Morel, Morel-Desrosiers, N. *J. Chem. Soc., Perkin Trans. 2* **2002**, 524−532; Arnaud-Neu, F.; Fuangswasdi, S.; Notti, A.; Pappalardo, S.; Parisi, M. F. *Angew. Chem.* **1998**, *110*, 120−122; *Angew. Chem., Int. Ed.* **1998**, *37*, 112−114.
(16) Ngola, S. M.; Kearney, P. C.; Mecozzi, S.; Russell, K.; Dougherty, D. A. *J. Am. Chem. Soc.* **1999**, *121*, 1192−1201.
(17) Bell, T. W.; Khasanov, A. B.; Drew, M. G. B.; Filikov, A.; James, T. *Angew. Chem., Int. Ed.* **1999**, *38*, 2543−2547.
(18) Famulok, M. *J. Am. Chem. Soc.* **1994**, *116*, 1698−1706.
(19) Two unspecifically binding calix[6]- and -[8]arene carboxylates were used to extract biologically active cytochrome *c* from water into chloroform: Oshima, T.; Goto, M.; Furusaki, S. *Biomacromolecules* **2002**, *3*, 438−444.
(20) Kamieth, M.; Klärner, F.-G. *J. Prakt. Chem.* **1999**, *341*, 245−251; review: Klärner, F.-G.; Kahlert, B. *Acc. Chem. Res.* **2003**, *36*, 919−932.
(21) Klärner, F.-G.; Benkhoff, J.; Boese, R.; Burkert, U.; Kamieth, M.; Naatz, U. *Angew. Chem.* **1996**, *108*, 1195−1198; Klärner, F.-G.; Burkert, U.; Kamieth, M.; Boese, R.; Benet-Buchholz, J. *Chem. Eur. J.* **1999**, *5*, 1700−1707.
(22) Jasper, C.; Schrader, T.; Panitzky, J.; Klärner, F.-G. *Angew. Chem., Int. Ed.* **2002**, *41*, 1355−1358.; Fokkens, M.; Jasper, C.; Schrader, T.; Koziol, F.; Ochsenfeld, C.; Polkowska, J.; Lobert, M.; Kahlert, B.; Klärner, F.-G. *Chem. Eur. J.* **2005**, *11*, 477−494.

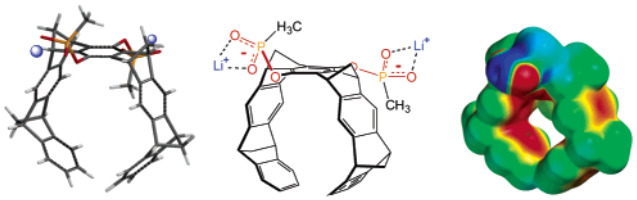

Figure 2. (Left) PM3 calculation of the bisphosphonate tweezer structure (syn−anti dilithium salt; $\Delta H^\circ_f = -163.5$ kcal/mol). (Right) Electrostatic potential surface calculated with PM3 showing the high electron density inside the tweezer cavity (MEP = −31.1 kcal/mol at asterisk; EPS color code: −25 kcal/mol: red; +25 kcal/mol: blue).

Table 1. Binding of Primary and Secondary Alkylammonium Guests by Bisphosphonate Tweezer **1**[a]

entry	guest-amine	$\Delta\delta_{sat}$ (ppm)[b]	K_a [M^{-1}] (%)	medium
1	benzyl-	1.5 (NCH_2)	120 ± 45	D_2O
2	propyl-	2.7 (NCH_2)$_2$	890 ± 11	K^1:D_2O
			1680 ± 9	K^2:MeOD
3	dop-	2.7 (NCH_2)$_2$	980 ± 13	D_2O
4	noradr.	0.9 (NCH_2)	180 ± 22	D_2O
5	adr.	2.1 (H_3CNCH_2)	390 ± 9	D_2O
6	propr.	0.5 (NCH)	precipitate	K^1:D_2O
			1360 ± 6	K^2:MeOD

[a] Dilution and conventional titrations at 0.1 mM. [b] Maximum shift predicted for 100% complexation from curve fitting.

weak K_D values in the millimolar regime (Table 1).[23] Both binding mode and strength seem to be largely governed by steric effects. Thus, bulky substituents (naphthyl, phenyl, isopropyl) close to the ammonium functionality prevent an effective inclusion into the tweezer cavity, so that upfield shifts and K_a values remain small (entries 1,4,6). On the contrary, the slim ethylammonium environment allows complete insertion into the host interior, accompanied with large upfield shifts and superior affinities (entries 2,3). Remarkably, unbranched secondary ammonium ions are likewise accommodated inside the receptor, as evidenced by the simultaneous shielding of both alkyl groups; clearly, adrenaline is bound with complete desolvation of its dialkylammonium moiety (entry 5). Obviously, this threading procedure takes advantage of not only π−cation stabilization but also substantial dispersive forces (Figure 3). α-*N/C*-Protected arginine and lysine are biologically interesting primary cations with slim alkyl residues, which fulfill the above-detailed requirements for efficient complexation by tweezer **1**. Surprisingly, their respective association constants in water proved to be at least 1 order of magnitude superior to those of simple alkylammonium ions ($K_a \approx 10^4$ M^{-1}). Extremely large upfield shifts are observed along the whole amino acid side chain, reaching far to the α-carbon (Figure 4). No other amino acid showed a comparable behavior, rendering the tweezer highly selective for basic amino acids (Table 2).[24]

Complex geometry and binding mode could be elucidated after thorough chemical shift analysis, NOESY and variable-temperature experiments; since the $\Delta\delta_{sat}$ values for lysine's δ and ϵ CH_2 groups exceed 3 ppm, they must both permanently

(23) Connors, K. A. *Binding Constants, The Measurement of Molecular Complex Stability*; Wiley: New York, 1987; Fielding, L. *Tetrahedron* **2000**, *56*, 6151−6170.

(24) Only histidine's imidazolium cation is bound with moderate affinity ($K_a \approx 700$ M^{-1}). The *N*-Ts group on Arg is larger than the *N*-acetyl groups on Lys and His; although no steric hindrance is observed in the modeling structure, it cannot be entirely ruled out that this size difference might to some extent account for its lower affinity towards the tweezer.

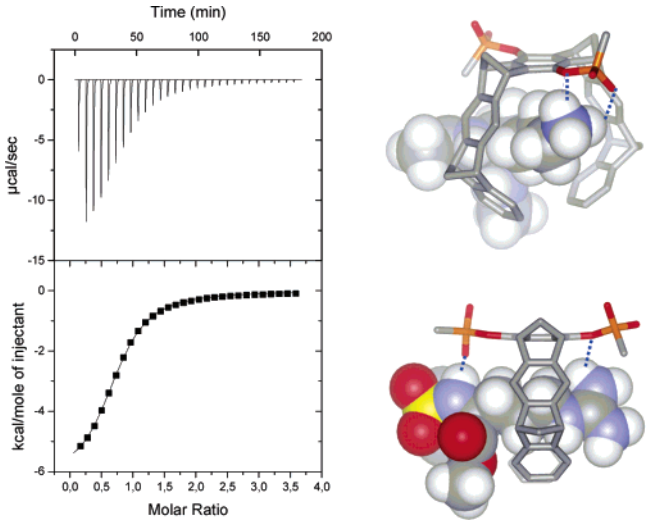

Figure 3. (Left) ITC titration curve for Ac-Lys-OMe and **1** in water. Note the strong exothermicity of the binding event. (Right) Monte Carlo simulations of the complexes between tweezer **1** and Ac-Lys-OMe (top) as well as Ts-Arg-OEt (bottom, MacroModel 7.1, Amber*, water, 5000 steps).[28]

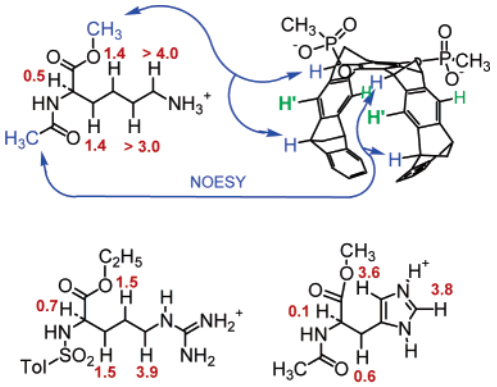

Figure 4. Upfield shifts of the guest protons (red), NOESY cross-peaks (blue) and host signal nonequivalence (green) due to chirality transfer in the complex between host **1** and *N/C*-protected lysine, arginine and histidine.

Table 2. Binding of Lysine- and Arginine-Containing Small Peptides by Bisphosphonate Tweezer **1**[a]

Guest	$\Delta\delta_{sat}$[b]	K_a [M^{-1}]	Sto.	medium
AcLys**OMe**	> 4 ppm (ε-H)	23000 ± 18%	1:1	D_2O
AcLys**OMe**	> 4 ppm (ε-H)	4400 ± 22%	1:1	25mM NaH_2PO_4
HLys**OH**	> 4 ppm (ε-H)	1400 ± 8%	1:1	25mM NaH_2PO_4
Ts**Arg**OEt	3.9 ppm (δ-H)	7800 ± 25%	1:1	D_2O
Ts**Arg**OEt	3.9 ppm (δ-H)	1800 ± 40%	1:1	25mM NaH_2PO_4
Ac**His**OMe	3.8 ppm (H_{ar})	700 ± 15%	1:1	25mM NaH_2PO_4
K-**A**-**A**	2.8 ppm (ε-H)	1200 ± 14%	1:1	25mM NaH_2PO_4
KKLVFF	0.2 ppm (ε-H)	38000 ± 33%	1:1	25mM NaH_2PO_4[c]
K**TT**K	2.8 ppm (ε-H)	5500[d] ± 31%	2:1[d]	25mM NaH_2PO_4
K**TTK**S	2.8 ppm (ε-H)	4200[d] ± 27%	2:1[d]	25mM NaH_2PO_4
RGD	4.6 ppm (δ-H)	1000 ± 9%	1:1	D_2O
RGD	4.6 ppm (δ-H)	1200 ± 16%	1:1	25mM NaH_2PO_4
G**R**GG	~ 4 ppm (δ-H)	900 ± 12%	1:1	25mM NaH_2PO_4

[a] Dilution and conventional titrations at 0.1 mM in D_2O and with 25 mM NaH_2PO_4 buffer (pH 7.0). [b] Maximum shift predicted for 100% complexation from curve fitting. [c] Due to KLVFF's low solubility, a 1:1 mixture betweeen D_2O and CD_3OD had to be used. [d] 2:1 complex between tweezer and peptide according to a Job plot ($K_{1:1}$ calculated for each single step, assuming no cooperativity).

reside inside the tweezer cavity.[25] However, the β and γ methylene protons also experience considerable shielding (~1.5 ppm) and hence must in part also be inserted into the aromatic cleft. A good explanation is a back-and-forth movement of the

extended alkyl chain, similar to that of the axis inside the wheel in "pseudorotaxanes".[26] In such a scenario, the ammonium group sticks out of the cavity and is ideally positioned for an effective salt bridge with a phosphonate tweezer, without the need of its own costly complete desolvation. At the other end, the branching at the α-carbon acts as a stopper to hold the "axle" in place inside its "bearing".[27] Remarkably, free lysine and even ϵ-Z-protected lysine ester with a neutral side chain both follow the same binding mechanism, indicating a substantial contribution of van der Waals interactions (Table 2).

Several pieces of experimental evidence support this picture. Concomitant with complexation, line-broadening of all four guest CH_2 signals is observed; it can be reverted at elevated temperatures without losing its strong upfield shift and thus indicates the decelerated rotation inside this bearing. A NOESY experiment revealed intermolecular cross-peaks exactly between the tweezer's bridgehead methine protons and lysine's *N/C*-terminal acetyl as well as methyl ester protons. These contacts can only occur in the above-detailed "pseudorotaxane" arrangement of host and guest. Both complex partners are interlocked so tightly that in the course of a chirality transfer the aromatic host protons become magnetically nonequivalent. Thus, efficient inclusion of the aliphatic amino acid side chain inside the tweezer's cavity leads to extensive van der Waals interactions, reinforced by electrostatic attraction between the cationic end group and the host's phosphonate anion. In addition, the "pseudorotaxane" is mechanically locked in form of the α-branching. This peculiar binding mechanism infers high selectivity for lysine and arginine derivatives onto the tweezer. Monte Carlo calculations with 3000 steps in a water environment reach the same complex geometry as the most stable arrangement for both basic amino acids.[28] In buffered solution (25 mM NaH_2PO_4), the binding free energy drops to half of its original value and confirms the substantial contribution of electrostatic attraction in the complex (Table 2). An ITC measurement confirms the extraordinary affinity of the tweezer for lysine, reaching a K_a value of 17000 M^{-1} at an approximate 1:1 stoichiometry with a dominating enthalpic contribution ΔH of −6.3 kcal/mol, overriding the entropy term $-T\Delta S$ of 0.7 kcal/mol. The remarkably exothermic character of the binding event correlates well with the assumed threading procedure and the resulting van der Waals interactions between host cavity and amino acid side chain.

The above-reported K_a values place host **1** among the most efficient receptor molecules for basic amino acids known today. In pure water, Bell's "arginine cork" binds free arginine with a K_a value of 900 M^{-1}.[17] The best calixarene host, a tetrasulfonate, reaches 1500 M^{-1} in borate buffer,[15] while Dougherty's cyclophane shows an affinity of 5000 M^{-1} toward Arg-NH_2 in the same medium,[16] only surpassed by Famulok's RNA aptamer with 13000 M^{-1}.[18] However, all these hosts bind lysine derivatives much more weakly, at most with a millimolar K_D.[16] To the best of our knowlege, we present here the most efficient artificial lysine binder, which is roughly 1 order of magnitude superior to all other receptor molecules that have hitherto been designed for this purpose. In a systematic variation of the annulated oligopyridine skeleton of the arginine cork, Bell later identified a selective lysine binder ($K_a > 10^5$ M^{-1} in methanol).[29] However, in water the host molecule aggregates due to extensive π-stacking between its large hydrophobic aromatic receptor faces; this effect is even significantly enhanced on addition of cationic guest molecules.

To extend the scope of the new molecular tweezer, we tested its ability to include basic amino acid side chains at different positions of small peptides. Biologically relevant examples included the arginine-based tripeptide RGD, responsible for many cell-surface recognition events. KAA, an important bacterial cell wall ingredient, and KKLVFF, the self-complementary central part of Alzheimer's peptide both contain *N*-terminal lysines, whereas in KTTKS, a regeneration signal of injured skin, one of the lysines is found in the middle of the peptide, clearly separated from the other one. These important signal peptides are all bound quite efficiently in buffered aqueous solution, irrespective of the amino acid's position within the peptide (*K*AA, *KK*LVFF, *K*TT*K*S, *R*GD, G*R*GG). In all cases but one, extremely large upfield shifts are observed exclusively at the δ- and ϵ-methylene protons of the basic amino acid side chains, confirming again the host's high selectivity for peptidic arginine and lysine.

Those peptides containing only one basic amino acid are bound a little more weakly in buffered aqueous solution than are their parent amino acid derivatives, possibly due to steric hindrance of the extended peptide backbone. KTTKS and KKLVFF with two lysines display an enhanced affinity toward host **1**, as expected. However, while a 2:1 stoichiometry is produced between receptor and KTTKS, which inserts both of its lysine residues into the host's cavities, only one tweezer molecule is needed to bind KKLVFF. Even more surprising is the drastic change in the binding mode: in KTTKS two tweezer molecules are able to embrace both lysine side chains (because these are spatially well separated), and a double "pseudorotaxane" structure with a peptidic axle is produced (Figure 5). By contrast, instead of alkylammonium inclusion, the *N*-terminal lysines in KKLVFF prefer multiple electrostatic attraction as they form a highly stable chelate cluster between all three of their NH_3^+ groups and the tweezers' phosphonate anions, indicated by minute chemical shift changes of both ϵ-CH_2's during the NMR titration. This striking difference can be regarded as an element of sequence selectivity, which is further supported by the slightly altered solvent environment: the highly unpolar *C*-terminal part of the KKLVFF sequence is only soluble in a 1:1 water/methanol mixture, whose lowered dielectric constant may in part contribute to the observed drastic change in the binding mode. However, lysine itself remains included in the clip cavity under these conditions (Figure 6.).

Remarkably, the tight grip around lysine's and arginine's alkyl side chain can be deliberately loosened if, instead of methanol,

(25) The experimental values could be compared with quantum chemical calculations supported by solid-state NMR experiments on related systems: Ochsenfeld, C.; Koziol, F.; Brown, S. P.; Schaller, T.; Seelbach, U. P.; Klärner, F.-G. *Solid State Nucl. Magn. Reson.* **2002**, *22*, 128−153.

(26) The word *pseudorotaxanes* is usually reserved for rotaxanes containing macrocycles (not tweezers) without stoppers at their chain ends. Related highly stable "pseudorotaxane" structures: Klärner, F. G.; Verhaelen, C.; Schalley, C. A.; Hahn, U.; Vögtle, F. *Angew. Chem., Int. Ed.* **2005**, *44*, 477−480.

(27) A structurally and functionally related host was recently studied by the Isaacs group: Burnett, C. A.; Witt, D.; Fettinger, J. C.; Isaacs, L. *J. Org. Chem.* **2003**, *68*, 6184−6191.

(28) Mohamadi, F.; Richards, N. G. J.; Guida, W. C.; Liskamp, R.; Lipton, M.; Caufield, C.; Chang, G.; Hendrickson, T.; Still, W. C. *J. Comput. Chem.* **1990**, *11*, 440−467.

(29) Bell, T. W.; Khasanov, A. B.; Drew, M. G. B. *J. Am. Chem. Soc.* **2002**, *214*, 14092−14103.

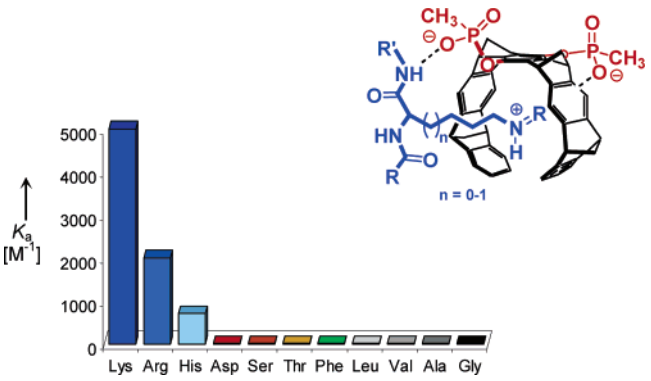

Figure 5. Selectivity of host **1** for *N/C*-protected amino acids: K_a values in buffered aqueous solution (c = 0.1 mM in 25 mM NaH_2PO_4, pH = 7.0). Due to the complete absence of any chemical shift changes with all but the basic amino acids, this value was set to 5 M^{-1} as an upper limit for all other candidates.

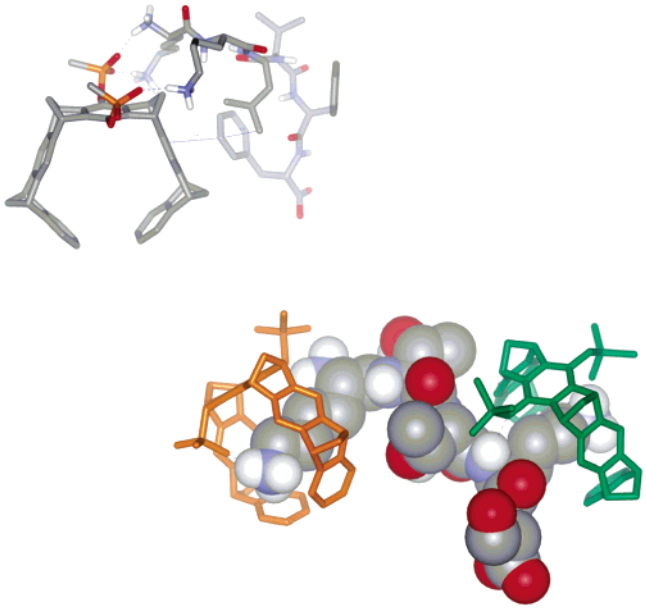

Figure 6. Proposed binding mode between tweezer **1** and KKLVFF (top) as well as KTTKS (bottom). *N*-terminal lysines prefer multiple salt bridges, whereas isolated lysines are both threaded through separate tweezer cavities, forming a double "pseudorotaxane" (MacroModel 7.0, water, Amber*, 10000 steps). Note the hydrophobic aggregate formed between the nonpolar extended LVFF fragment and the tweezer's aromatic sidewall.

a dipolar aprotic solvent is added to the complex. Due to its nonpolar interior, DMSO and acetonitrile prefer to insert their methyl groups into the cavity and replace the guest. It is completely released into solution, as indicated by a total reversion of chemical shift changes to the peptide's free state after addition of ~1000 equiv of DMSO. By a simple change of cosolvent composition, the complexation process can hence be switched on and off —in a very mild manner.[30,31]

Outlook. We are currently further modifying the simple basic structure of receptor **1** by incorporation of recognition sites for other amino acid side chains. Thus, specific host molecules for the RGD as well as the KAA and KKLVFF sequence are envisaged, designed as sensors, molecular probes and potential drugs with— hopefully —unprecedented specificity and biological activity.

(30) Similar observations concerning the solvent dependence have been made with immobilized tweezers: Kamieth, M.; Burkert, U.; Corbin, P. S.; Dell, S. J.; Zimmerman, S. C.; Klärner, F.-G. *Eur. J. Org. Chem.* **1999**, 2741–2749.

(31) It should be possible to turn the binding event back on either by dialysis or by lyophyllization and redissolution in pure aqueous buffer.

Experimental Section

9,10-*O,O′*-Bis(methylmethoxyphosphoryloxy)-(1α,1α,5α,8α)-1,1,5,8-tetrahydro-1,1:5,8-dimethanoanthracene 1a.

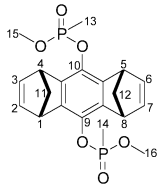

Syn-9,10-dihydroxy-(1α,4α,5α,8α)-1,4,5,8-tetrahydro-1,4:5,8-dimethanoanthracene (200 mg, 0.85 mmol) and methanephosphonic acid dichloride (297 mg, 2.27 mmol) are dissolved in dry THF (15 mL), and triethylamine (350 μL, 2.50 mmol) is added dropwise at 0 °C. Stirring is continued for 1 h at 0 °C and for another 1 h at ambient temperature. Then dry methanol (10 mL) is added, and the mixture is stirred for another 16 h at room temperature. Subsequently, the solvent is removed under reduced pressure, and the resulting solid is purified by chromatography over silica gel eluting with chloroform/acetone = 2:1 v/v. Yield 234 mg (0.56 mmol, 65%), colorless solid; mp 139 °C; R_f 0.25 in chloroform/acetone = 2:1 v/v. ^{1}H NMR (300 MHz, methanol-d_4): δ = 1.68 (d, ^2J(13-H, P) = 17.3 Hz, 6 H, 13-H, 14-H), 2.19 (d br, ^2J(11-H^i, 11-H^a) = 7.0 Hz, 2 H, 11-H^i, 12-H^i), 2.25 (d, ^2J(11-H^a, 11-H^i) = 7.0 Hz, 2 H, 11-H^a, 12-H^a), 3.75 (d, ^3J(15-H, P) = 11.3 Hz, 6 H, 15-H, 16-H), 4.11 (d br, ^3J(1-H, 2-H) = 1.7 Hz, 4 H, 1-H, 4-H, 5-H, 8-H), 6.83 (d br, ^3J(2-H, 1-H) = 1.7 Hz, 4 H, 2-H, 3-H, 6-H, 7-H). ^{31}P NMR (81 MHz, $CDCl_3$): δ = 29.33 (s). ^{13}C NMR (50.3 MHz, $CDCl_3$): δ = 10.8 (d, ^1J(C, P) = 144.3 Hz, C-13, C-14), 48.1 (d, C-1, C-4, C-5, C-8), 52.7 (d, ^2J(C, P) = 5.4 Hz, C-15, C-16), 70.0 (s, C-11, C-12), 136.2 (d, C-4a, C-8a, C-9a, C-10a), 142.3–142.8 (m, C-2, C-3, C-6, C-7, C-9, C-10). MS (ESI, MeOH); *m/z*: 423 [M + H$^+$]$^+$, 445 [M + Na$^+$]$^+$; HRMS for $C_{20}H_{24}O_6NaP_2$: calcd 445.0946, found 445.0940; elemental analysis for $C_{20}H_{24}Li_2O_6P_2 \cdot {}^1/_2H_2O$: C 55.69, H 5.84; found: C 55.15, H 5.55.

Bis(lithium)-1,1,5,8-tetrahydro-1,1,5,8-dimethanoanthracene-9,-10-bismethylphosphonate 1b.

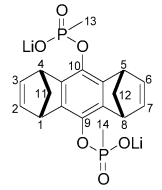

1a (50.0 mg, 1.18 mmol) and dry LiBr (20.5 mg, 2.36 mmol) are dissolved in dry acetonitrile (10 mL) and stirred for 16 h at 85 °C. The resulting precipitate is collected by centrifugation, washed thrice with dry acetonitrile (3 mL) and dried in vacuo. Yield 35 mg (0.86 mmol, 73%), colorless solid; mp >230 °C; ^{1}H NMR (500 MHz, methanol-d_4): δ = 1.27 (d, ^2J(13-H, P) = 16.5 Hz, 6 H, 13-H, 14-H), 2.15 (s br, 4 H, 11-H, 12-H), 4.16 (s br, 4 H, 1-H, 4-H, 5-H, 8-H), 6.78 (s br, 4 H, 2-H, 3-H, 6-H, 7-H); ^{31}P NMR (81.0 MHz, methanol-d_4): δ = 25.3 (s); ^{13}C NMR (125.8 MHz, methanol-d_4): δ = 13.3 (d, ^1J(C, P) = 138.3 Hz, C-13, C-14), 70.6 Hz (s, C-11, C-12), 139.6 (d, ^2J(C, P) = 6.1 Hz, C-9, C-10), 143.3 (s, C-4a, C-8a, C-9a, C-10a), 144.1 (s, C-2, C-3, C-6, C-7); MS (ESI, MeOH); *m/z*: 196 [M − 2Li$^+$]$^{2-}$, 393 [M − 2Li$^+$ + H$^+$]$^-$, 399 [M − Li$^+$]$^-$. HRMS for $C_{18}H_{18}O_6LiP_2$: calcd 399.0733, found 399.0709; elemental analysis for $C_{18}H_{18}Li_2O_6P_2 \cdot 2H_2O$: C 48.89, H 5.01; found: C 49.10; H 5.00.

8,19-*O*,*O*′-Bis(methylmethoxyphosphoryloxy)-(5α,7α,9α,11α,-16α, 18α,20α,22α)-5,7,9,11,16,18,20,22-octahydro-5,22:7,20:9,18:11,-16-tetramethanononacene 1c.

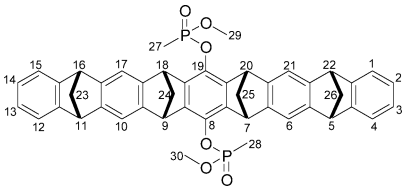

The hydroquinone tweezer[2, 3] (82 mg, 0.144 mmol) and methanephosphonic acid dichloride (48 mg, 0.36 mmol) are dissolved in dry THF (10 mL), and triethylamine (60 μL, 0.43 mmol) is added dropwise at 0 °C. Stirring is continued for 1 h at 0 °C and for another 1 h at ambient temperature. Then dry methanol (3 mL) is added, and the mixture is stirred for another 16 h at room temperature. Subsequently, the solvent is removed under reduced pressure, and the resulting solid is purified by chromatography over silica gel eluting with chloroform/acetone = 20:1 v/v. Yield 60 mg (0.08 mmol, 56%), colorless solid; R_f 0.62 in chloroform/acetone = 3:1 v/v. The byproduct methanephosphonic acid methyl ester is removed by prolonged heating in vacuo at 50 °C. ^{1}H NMR (300 MHz, methanol-d_4): δ = 1.62 (d, ^2J(27-H, P) = 17.9 Hz, 6 H, 27-H, 28-H), 2.30−2.40 (m, 8 H, 23-H, 24-H, 25-H, 26-H), 2.52, 2.54 (2 d, ^3J(29-H, P) = 11.3 Hz, 6 H, 29-H, 30-H), 4.04, 4.07 (2 d, ^3J(5-H, 26-H) = 7.0 Hz, 4 H, 5-H, 11-H, 16-H, 22-H), 4.26, 4.36 (2 d, ^3J(7-H, 25-H) = 4.3 Hz, 4-H, 7-H, 9-H, 18-H, 20-H), 6.66−6.82 (m, 4 H, 2-H, 3-H, 13-H, 14-H), 6.95−7.08 (m, 4-H, 1-H, 4-H, 12-H, 15-H); ^{31}P NMR (81 MHz, $CDCl_3$): 29.07 (s); ^{13}C NMR (75.5 MHz, $CDCl_3$): δ = 11.5 (2 d, ^1J(C, P) = 148.1 Hz, C-27, C-28), 48.7, 48.9 (2 d, C-7, C-9, C-18, C-20), 51.2 (s br, C-29, C-30), 52.1, 52.2 (2 s, C-5, C-11, C-16, C-22), 67.8 (m, C-24, C-25), 68.9 (m, C-23, C-26), 116.7, 117.6 (2 d, C-6, C-10, C-17, C-21), 121.0, 121.1 (2 d, C-1, C-4, C-12, C-15), 124.6, 124.8 (2 d, C-2, C-3, C-13, C-14), 136.3 (s, C-8, C-19), 142.2, 142.4 (2 d, ^3J(C, P) = 17.0 Hz, C-7a, C-8a, C-18a, C-19a); MS (ESI, MeOH); *m*/*z*: 752 [M + H$^+$]$^+$, 773 [M + Na$^+$]$^+$, 789 [M + K$^+$]$^+$; HRMS for $C_{46}H_{41}O_6P_2$: calcd 751.2373, found 751.2374.

Bis(lithium)-(5α,7α,9α,11α,16α,18α,20α,22α)-5,7,9,11,16,18,20,-22-octahydro-5,22:7,20: 9,18:11,16-tetramethanononacene-8,19bis-methylphosphonate 1.

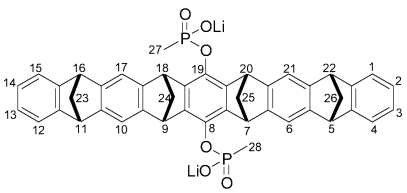

1c (30.0 mg, 0.40 mmol) and dry LiBr (10 mg, 0.12 mmol) are dissolved in dry acetonitrile (10 mL) and stirred for 16 h at 85 °C. The resulting precipitate is collected by centrifugation, washed thrice with dry acetonitrile (2 mL) and dried in vacuo. Yield 23.4 mg (0.32 mmol, 80%), colorless solid; mp >230 °C; ^{1}H NMR (300 MHz, D_2O): δ = 1.30 (d, ^2J(27-H, P) = 16.2 Hz, 6 H, 27-H, 28-H), 2.31 (d, ^2J(24-H^a, 24-H^i) = 8.0 Hz, 2 H, 24-H^a, 25-H^a), 2.33−2.36 (m, 4 H, 23-H, 26-H), 2.47 (d, ^2J(24-H^i, 24-H^a) = 7.6 Hz, 2 H, 24-H^i, 25-H^i), 4.16 (s, 4 H, 5-H, 11-H, 16-H, 22-H), 4.38 (s, 4 H 7-H, 9-H, 18-H, 20-H), 6.29 (s br, 2-H, 3-H, 13-H, 14-H), 7.01−7.04 (m, 4 H, 1-H, 4-H, 12-H, 15-H), 7.29 (s, 4 H, 6-H, 10-H, 17-H, 21-H); ^{31}P NMR (81.0 MHz, D_2O): δ = 25.99 (s); ^{13}C NMR (125.6 MHz, methanol-d_4): δ = 13.4 (d, ^1J(C, P) = 138.4 Hz, C-27, C-28), 50.0 (s, C-7, C-9, C-18, C-20), 52.4 (s, C-5, C-11, C-16, C-22), 68.9 (s, C-24, C-25), 69.4 (s, C-23, C-26), 117.3 (s, C-6, C-10, C-17, C-21), 122.0 (s, C-1, C-4, C-12, C-15), 125.8 (s, C-2, C-3, C-13, C-14), 138.9 (d, ^2J(C, P) = 8.1 Hz, C-8, C-19), 142.8 (s, C-7a, C-8a, C-18a, C-19a), 148.6 (s, C-6a, C-9a, C-17a, C-20a), 149.3 (s, C-5a, C-10a, C-16a, C-21a), 152.0 (s, C-4a, C-11a, C-15a, C-22a); MS (ESI, MeOH); *m*/*z*: 360 [M − 2Li$^+$]$^{2-}$, 727 [M − Li$^+$]$^-$; HRMS for $C_{44}H_{34}O_6LiP_2$: calcd 727.1985, found 727.1985.

NMR Titrations at Constant Guest Concentration. Ten NMR tubes are filled with the same amount of guest solution in deuterated solvent. Subsequently the host solution in the same deuterated solvent is added successively in increasing amounts to tubes 2−10. All NMR tubes are filled with deuterated solvent to the same total volume, to avoid dilution-induced CIS on the guest. NMR tube 1 is the reference sample. The guest concentration should ideally match the expected dissociation constant of the complex. In addition, one sample of a 1:1 mixture between guest and model host compound **2** is always prepared in the same deuterated solvent and concentration range to be able to distinguish between nonspecific binding and specific guest inclusion inside the cavity of **1**. Calibrations of all spectra were performed with the rest proton signal of the respective deuterated solvent. Binding constants and $\Delta\delta_{sat}$ values of all observed NMR signals were obtained by nonlinear regression analysis.

For every titration with constant guest concentrations, the concentrations of host and guest as well as the added volumes and the amount of solvent necessary to reach the same total end volume are given in the tables in Supporting Information. The absolute chemical shifts of all signals involved in the complexation process are given, followed at the end by the respective binding constants and the calculated $\Delta\delta_{sat}$ values.

Dilution Titrations. Host and guest are dissolved at an approximate 1:1 ratio in a deuterated solvent. An NMR spectrum is measured. Subsequently this solution is diluted several times with deuterated solvent and an NMR spectrum is measured at each dilution step. To ensure, that the observed chemical shift changes are indicative of the complexation process, a host and a guest solution are likewise diluted stepwise, and measured at some of the concentrations, described for the complex titration outlined above. Only those signals can be evaluated which do not show any chemical shift change on dilution of both pure host and pure guest compound. Similar to conventional titrations at constant concentrations, even in the case of dilution titrations, the guest is added at an approximate 1:1 ratio to model compound **1** in the same deuterated solvent, to exclude nonspecific interactions other than inclusion inside the cavity. Again, all NMR spectra are calibrated onto the rest proton signal of the respective solvent. Binding constants and $\Delta\delta_{sat}$ values of all observed NMR signals were obtained by nonlinear regression analysis. For every dilution titration the amounts of guest and host are given in the tables in Supporting Information, accompanied by the dilution steps of the parent solution (sample 1) as well as the absolute chemical shift values of all observed NMR signals. The calculated binding constants and $\Delta\delta_{sat}$ values are given at the end of each table. Error margins represent the mathematical error from curve-fitting; at least 2−3 different NMR signals were observed and evaluated simultaneously for each guest compound, giving an averaged K_a value.

Job Plots. The samples from the conventional NMR titrations with constant concentrations and varying host and guest ratios were used for the indirect determination of the complex stoichiometries from their respective molar fractions. These were multiplied with $\Delta\delta$ and plotted against the molar fraction itself.[4] Maxima indicate the molar fraction of host or guest which produces the largest complex concentration and therefore simultaneously indicates the complex stoichiometry.

NOESY Experiments. An equimolar solution (ca. 10^{-3} M) of host and guest in deuterated solvent was degassed by sonication and subjected to a standard NOESY experiment. Standard ^{1}H NOESY experiments were performed with host **1** in its complex with acetyl-(*S*)-lysine methyl ester hydrochloride on a Bruker 500 MHz NMR spectrometer. Mixing times varied between 100 and 200 ms. Positive reciprocal NOE peaks were classified as w = weak, m = medium and s = strong.

Variable-Temperature Experiments. ^{1}H NMR spectra were measured from equimolar solutions (ca. 10^{-3} M) of host and guest in deuterated solvent (D_2O) in the temperature range from 5 to 95 °C in steps of 10 °C. The temperature-dependent change of the chemical shift was monitored, using the untouched aliphatic protons as internal reference.

ITC Measurements. ITC experiments were carried out on a Microcal VP-ITC. Titrations were performed at 298 K with a reference power of 10 μCal/s. The host concentration in the cell was set at 0.5 mM, and the guest was added through the syringe (7.5 mM) in 10 μL steps (5 μL for the first step) during 8 s (4 s for the first step). Spacings of 360 s between the single titration steps were applied.

Molecular Modeling. The program MacroModel 7.1 was used for model-building procedures and as graphical interface. Force-field parameters were taken from the built-in force fields, Amber* was chosen for all minimizations and Monte Carlo simulations. Minimizations and Monte Carlo simulations were carried out in aqueous solution. Energy minimizations were conducted over 1000 iterations on a Silicon Graphics O2 workstation. The best structures were subjected to conformational searches with 5000- or 10000-step Monte Carlo simulations.

Supporting Information Available: NMR titration curves, maximum CIS and derived binding constants, Job plots, ITC experiments, solvent titrations. This material is available free of charge via the Internet at http://pubs.acs.org.

JA052806A